



HAL
open science

Microstructural characterization of IN625 - NiCrAlY bond coat system fabricated by additive manufacturing

Fransiskus Damanik, Deni Ferdian, Dedi Priadi, Donanta Dhaneswara

► **To cite this version:**

Fransiskus Damanik, Deni Ferdian, Dedi Priadi, Donanta Dhaneswara. Microstructural characterization of IN625 - NiCrAlY bond coat system fabricated by additive manufacturing. I-MAMM 2020 - International meeting on advances in metallurgy and materials, Nov 2020, Depok, Indonesia. pp.080006-1 - 080006-6, 10.1063/5.0137035 . hal-04098961

HAL Id: hal-04098961

<https://imt-mines-albi.hal.science/hal-04098961v1>

Submitted on 16 May 2023

HAL is a multi-disciplinary open access archive for the deposit and dissemination of scientific research documents, whether they are published or not. The documents may come from teaching and research institutions in France or abroad, or from public or private research centers.

L'archive ouverte pluridisciplinaire **HAL**, est destinée au dépôt et à la diffusion de documents scientifiques de niveau recherche, publiés ou non, émanant des établissements d'enseignement et de recherche français ou étrangers, des laboratoires publics ou privés.

Microstructural Characterization of IN625 - NiCrAlY Bond Coat System Fabricated by Additive Manufacturing

Fransiskus Damanik^{1, 2, a)}, Deni Ferdian^{1, b)}, Dedi Priadi^{1, c)} and Donanta Dhaneswara^{1, d)}

¹*Dept. of Metallurgy and Materials Engineering, Universitas Indonesia, Kampus Baru UI Depok, 16424, Indonesia*

²*Institut Clément Ader (ICA), Université de Toulouse, CNRS, IMT Mines Albi, INSA, ISAE-SUPAERO, UPS, Campus Jarlard, F-81013 Albi, France*

^{a)}*corresponding author: fransiskus_gandamana.damanik@mines-albi.fr*

^{b)} *deni@metal.ui.ac.id,*

^{c)} *dedi@metal.ui.ac.id*

^{d)} *donanta.dhaneswara@ui.ac.id*

Keywords: Nickel based Superalloy, Thermal barrier coating, MCrAlY bond coat, Additive manufacturing, Selective laser melting

Abstract. This research is conducted on the IN625 superalloy as a substrate fabricated by selective laser melting method, which is coated with bond coat. The microstructure and chemical composition are investigated using optical microscopy and Field Emission Scanning Electron Microscopy (FE-SEM) coupled to an Energy Dispersive Spectroscopy (EDS) detector. The bond coat and substrate present a homogeneous microstructure, strong metallurgical bond and good adherence between substrate and bond coat. Moreover, the microstructure is difficult to distinguish between the bond coat and substrate using optical microscopy. Furthermore, the selective laser melting has a low level of Oxygen, indicating a low diffusion and oxidation rate during manufacturing process.

1. INTRODUCTION

The turbine blade has the function to transform the amount of kinetic energy of waste gases to be the amount of the effort which can operate the compressor and other components. Due to its function, the turbine blades are subjected to high stress and temperature which can be higher than 1150 °C. So far, IN625 constitutes one type of Nickel-based superalloy that compatible with those conditions. IN625 is Nickel robust solution strengthening superalloy that combines high tensile strength, creep strength, rupture strength, excellent fatigue, and oxidation resistance at high temperatures. The combination of those properties cannot be separated from the influence of the alloying elements [1].

The development of IN625 for the turbine blades, for which it was not meant to be used, makes the use of protection system necessary. Thermal barrier coating (TBC) is the best solution for a high-temperature application so far. Typical thermal barrier coating consists of MCrAlY or (Ni, Pt) Al bond coat layer combined with thermally insulative top coat made, yttria-stabilized zirconia $ZrO_2 - 8wt.\% Y_2O_3$. During the oxidation reaction at high temperature, a thin layer Thermally Grown Oxide (TGO) forms between TBC and MCrAlY bond coat [2, 3, 4]. TGO is a protective, stable, and alumina scale with good adherence. For typical MCrAlY bond coat, M is either nickel or cobalt or a combination of the two, and Yttrium (Y) is a reactive element added in minor proportions [2, 5, 6, 7], which contributes to the alumina scale adhesion, growth, and microstructure when the substrate is oxidized [2, 3, 4, 8, 9].

The selective laser melting (SLM) process has been widely used for fabricating IN625. It employs a laser beads to melt pure metal or pre-alloyed powders layer by layer according to given Computer-Aided Design

(CAD) model. The process can create nearly fully dense metal parts with complex geometries and material saving [10, 11, 12]. SLM parts have characteristics such as near-net-shape and good metallurgical bonding between each layer due to significant remelting of previously solidified layers [13]. The tensile strength of as-build IN625 is much higher than wrought standard level due to the influence of the very fine microstructure obtained from the different scanning strategies [14, 15]. Besides, SLM parts often exhibit out-of-equilibrium microstructure and strong anisotropy due to the directional columnar grain growth caused by directional thermal conduction during the SLM process [16, 17].

The sample for this study was IN625 coated by NiCrAlY. IN625 was fabricated using Selective Laser Melting (SLM), while NiCrAlY bond coat was deposited using the same process. This study will analyze the microstructure and chemical composition of sample, particularly the Oxygen content that affects the microstructure and characteristics of SLM parts resulting.

2. EXPERIMENTAL PROCEDURES

2.1 Materials and Processes

This study used IN625 fabricated by the Selective Laser Melting (SLM) process, subsequently coated with NiCrAlY using the same process. The chemical composition of IN625 powder is shown in Table 1 and Table 2. The powder is heated at 200°C for 24 hours before the SLM process. The heating process purposes of eliminating the water vapour inside the powder and improving the flowability of the powder. The IN625 was fabricated using 400 W fibre laser, which laser spot is 70 µm in diameter, and scanning speed range 200-1000 mm/s. High purity argon gas atmosphere is used to limit oxidation during the process (partial pressure Oxygen kept under 0.1 wt% during the process). Sample consisted of 30 x 20 x 2.6 mm coupons IN625 with a bond coat thickness of approximately 30µm.

TABLE 1. Chemical composition of IN625 Superalloy powder [SLM Solution Group AG].

		Nominal composition (wt.%)													
		Ni	Cr	Mo	Nb	Fe	Ti	Al	Co	C	Ta	Si	P	Mn	S
IN625	Min (%)	Balance	20	8	3.15	-	-	-	-	-	-	-	-	-	-
	Max (%)		23	10	4.15	5	0.4	0.4	1	0.1	0.15	0.5	0.02	0.5	0.015

TABLE 2. Chemical composition of NiCrAlY bond coat powder [SLM Solution Group AG].

		Nominal composition (wt.%)				
		Al	Cr	Ni	O ₂	Y
NiCrAlY	Min (%)	9	21	Balance	-	0.8
	Max (%)	11	23		0.05	1.2

2.2 Microstructures

The cross-section of all coated samples was ground using 1200 grit SiC abrasive paper, then polished using the alumina suspension and diamond paste of 0.1µm, and subsequently cleaned in acetone. Afterwards, all samples were electro-etched using a solution of 80 ml H₃PO₄ with 10 ml H₂O at 3V for 9 s. Microstructural observation were performed by using a FE-SEM Inspect F50. FE-SEM was equipped with an energy dispersive X-ray spectrometry detector (EDS) for micro-chemical composition analysis. Surface morphology was observed with an optical microscopy.

3. RESULT AND DISCUSSION

3.1 Microstructure and Characteristic of SLM Sample

The morphology of the samples was investigated using the optical microscopy, as shown in figure 1, and using scanning electron microscopy, as shown in figure 2. The laser beads in the form of the line that were parallel to other laser beads. Many parallel laser beads tend to look like hatching. The adjacent melting tracks tightly overlap, with a width of approximately 10 μm , generating nearly full dense-structure devoid lacuna, while the laser track length of roughly 25 μm . Therefore, it confirms that IN625 superalloy powder has an excellent forming performance [14, 15]. The irregular spheres were found among the laser beads. The presence of the molten pool was highly related to laser beads heat source and laser movement speed. The powder was continuously melted in the front of the molten pool, and the melted metal liquid rapidly solidified as soon as the laser moves away [11]. The laser beads presented in figure 1(a) indicate that morphology of the layer overlaps each other.

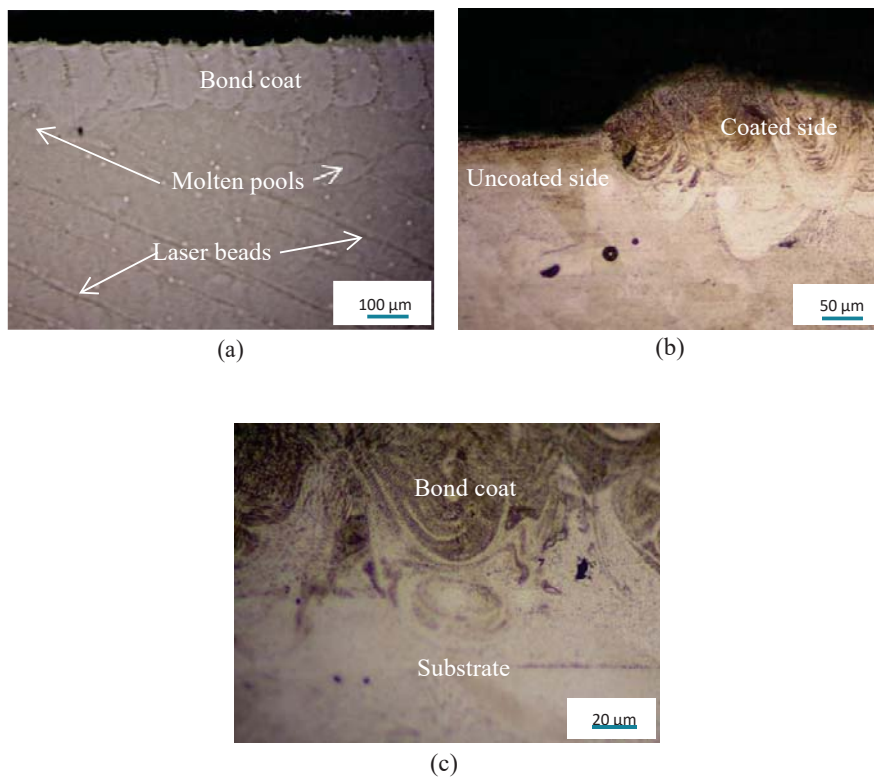


FIGURE 1. Metallographic image of cross-section: (a) molten pool without the etching process, (b) coated and uncoated side after etching process, (c) bond coat and substrate with the etching process.

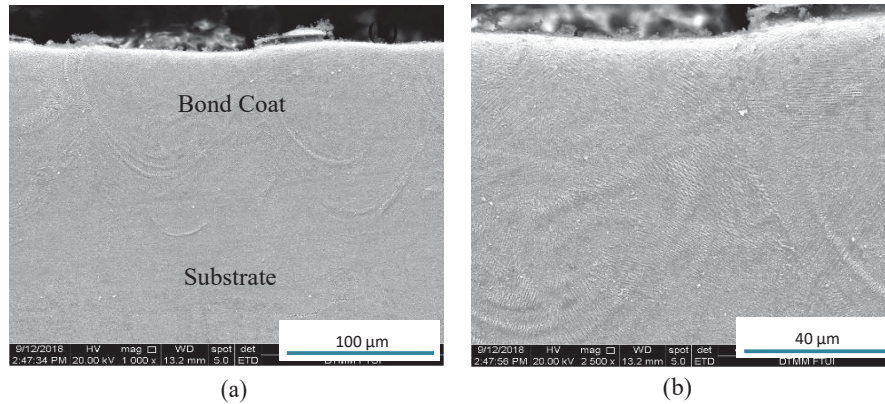


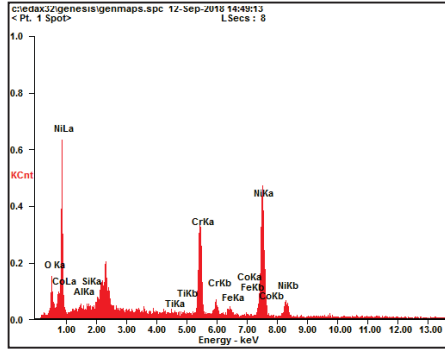
FIGURE 2. SEM micrograph of cross-section: (a) Difference substrate and between bond coat area, (b) High magnification of the bond coat area.

The difference is visible between coated and uncoated surface, as shown in figure 1(b). At a glance, bond coat has different laser beads with the substrate, where the hatching direction is almost perpendicular to the hatching direction of the substrate. Even, after polishing sometimes, the difference between the bond coat and the substrate was not clear, so that it is necessary to etch using compatible etchant. The difficulty of distinguishing between the substrate and bond coat is due to several factors. Namely, most of the constituent elements of the substrate and bond coat were similar, the fabrication of the substrate and the deposition of the bond coat using selective laser melting process, led to a strong atomic metallurgical bond between the substrate and bond coat [13]. Strong metallurgical bond sign a little Ar gas entrapment during SLM process. The last two factors are related to the process parameter of selective laser melting used, including laser beads speed, layer thickness, hatching distance, stripes pattern, powder morphology etc. Figure 1(b) and (c) displays the microstructure of substrate more white matrix γ -Ni dendritic phase due to the presence of Co and Cr elements, while microstructure of bond coat generates more black β -NiAl interdendritic phase due to higher Al content [9, 18].

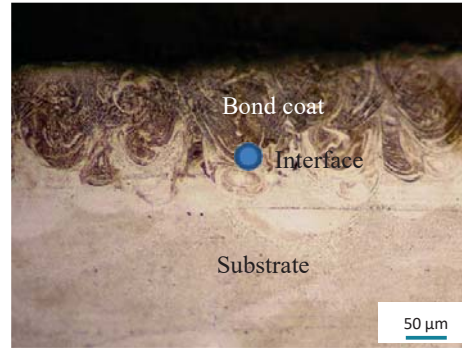
Metallography observation of substrate shows the overlapping molten pools and irregular laser beads, which is similar the bond coat. The difference of substrate both samples would be the laser beads and molten pools resulted. The microstructure of the substrate and bond coat consists of elongated dendrite and spherical cellular structures, as shown in figure 1(c) [16, 17, 19]. The dendrite structures indicate a high cooling rate where fine dendrites generate the fully dense and compact structure. Eventually, the fully dense and compact structure shows the strong atomic metallurgical bond in the substrate. The spherical cellular structures are a result of lower cooling rate [19].

3.2 Energy Dispersive Spectroscopy Analysis

The Energy dispersive spectroscopy analysis is focused in three areas that are bond coat, interface and substrate, as shown in figure 3. Ni and Cr are dominant content elements in the bond coat, interface and substrate. Moreover, the content of Ni and Cr do not change much. It indicates that there may not be a compound formed containing both elements [3, 4]. The mixing of elements such as Co, Al, Y, Fe, and O₂ with Ni-Cr shows a gradual variation of composition influenced by the microstructure obtained. The little amount of the Oxygen reacting/involving during fabrication of the substrate and deposition of the bond coat constitutes of the SLM parts characteristic. The energy dispersive spectroscopy analysis does not show any Yttrium content because of the low Yttrium powder content of less than 1%. Nevertheless, Yttrium has the similar effect with Oxygen in maintaining good adherence and strong atomic metallurgical bond, especially when influencing the high-temperature oxidation [3, 4, 5, 8].



(a)



(b)

Area	Ni (wt.%)	Cr (wt.%)	Al (wt.%)	Fe (wt.%)	O ₂ (wt.%)
Bond coat	64.42	22.05	2.07	-	7.4
Interface	64.44	22.46	2.07	2.63	6.43
Substrate	67.19	23.3	-	2.56	4.88

FIGURE 3. EDS micro-analysis of the phases taken from BSE image. (a) spectrum analysis for bond coat area, (b) SEM image correspond to the EDS analysis.

4. CONCLUSION

The microstructural characterization of bond coat used for high-temperature turbine blade application is investigated using optical microscopy, FE-SEM, and EDS. The substrate and bond coat can not be distinguished using scanning electron microscopy, but using optical microscopy with the etching process. The substrate and bond coat present a homogeneous microstructure, such as elongated dendrite and spherical cellular structure. The difficulty of distinguishing between the substrate and bond coat is due to several factors. Namely, most of the elements making up the substrate and bond coat are similar, selective laser melting method is used to fabricate the substrate and deposit the bond coat, the strong atomic metallurgical bond between the substrate and bond coat. The energy dispersive spectroscopy analysis presents the low Oxygen content of SLM parts.

ACKNOWLEDGMENTS

The authors would like to thank Institut Clément Ader (ICA), Université de Toulouse for the sample preparation. The financial support by Universitas Indonesia through Hibah Publikasi Internasional Terindeks Untuk Tugas Akhir (PITTA-Scheme A) 2019, contract No. NKB 0459/UN2.R3.1/HKP.05.00/2019 is highly appreciated.

REFERENCES

1. V. Shankar, S. K. B. Rao and S.L. Mannan, "Microstructural and Properties of Inconel 625," (Elsevier, Kalpakam, 2001), pp. 222-232.
2. R. C. Reed, "The Superalloys: Fundamentals and Application," Cambridge University Press, London (2006).
3. D. J. Young, "High-Temperature Oxidation and Corrosion of Metals," *Corrosion Series, First vol.*, Elsevier, Sydney (2008).
4. N. Birk and G.H. Meier, "Introduction of High-Temperature Oxidation of Metals," Cambridge University Press, London (1983).
5. N. Czech and W. Stamm, "Optimisation of MCrAlY-Type coatings for single crystal and conventional cast gas turbine blades," in *High Temperature Surface Engineering*, edited by J. Nicholls and D. Rickerb (Taylor & Francis Group, London, 2000), pp. 61-65.

6. D. R. G. Archer, R. Munoz-Arroyo, L. Singheiser and W. J. Quadackers, "Modelling of Phase Equilibria in MCrAlY Coating Systems," (Elsevier, Chennai, 2004), pp. 272–283.
7. S. Bose and J. Demasi-Marcin, Thermal Barrier Coating Experience in Gas Turbine at Pratt and Whitney, Thermal Barrier Coating Workshop, NASA CP 3312, National Aeronautic Space Administration 63 (1995).
8. S. Stecura, "Effects of Yttrium, Aluminum and Chromium Concentrations in Bond Coatings on the Performance of Zirconia-Yttria Thermal Barriers," (Elsevier, San Diego, 1980), pp. 481–489.
9. J. C. Pereira, J. C. Zambrano, E. Rayon, A. Yanez and V. Amigo, "Mechanical and Microstructural Characterization of MCrAlY Coatings Produced by Laser Cladding: The Influence of the Ni, Co and Al Content," (Elsevier, Gipuzkoa, 2018), pp. 22–31
10. M. M. Attallah, R. Jennings, X. Wang and L. N. Carter, "Additive Manufacturing of Ni-Based Superalloy : The Outstanding Issues," Cambridge University Press, London (2016).
11. S. Li., Q. Wei, Y. Shi, C. K. Chua, Z. Zhu and D. Zhang, Microstructure Characteristics of Inconel 625 Superalloy Manufactured by Selective Laser Melting," (Elsevier, Wuhan, 2015), pp. 946 – 952.
12. O. G. Rivera, P. G. Alisson, J. B. Jordon, O. L. Rodriguez, L. N. Brewer, Z. McClelland, W. R. Whittington, D. Francis, J. Su, R. L. Martens and N. Hardwick, "Microstructures and Mechanical Behavior of Inconel 625 Fabricated by Solid-State Additive Manufacturing," (Elsevier, Tuscaloosa, 2017), pp. 1 – 9.
13. M. Ansari, R. Shoja-Razavi, M. Barekat and H. C. Man, "High-Temperature Oxidation Behavior of Laser-Aided Additively Manufactured NiCrAlY Coating," (Elsevier, Najafabad, 2017), pp. 168–177.
14. H. Hack, R. Link, E. Knudsen, B. Baker and S. Olig, "Mechanical properties of additive manufactured Nickel alloy 625," (Elsevier, Annapolis, 2017), pp. 105-115.
15. C. P. Paul, P. Ganesh, S. K. Mishra, P. Bhargava, J. Negi and A. K. Nath, "Investigating Laser Rapid Manufacturing for Inconel-625 Components," (Elsevier, Indore, 2007), pp. 800-805.
16. C. Li, Y. B. Guo, J. B. Zhao, "Interfacial Phenomena and Characteristics Between the Deposited Material and Substrate in Selective Laser Melting Inconel 625," (Elsevier, Tuscaloosa, 2017), pp. 269-281.
17. C. Labre, A. L. Pinto and L. G. Solorzano, "Microstructure Evolution of Ni-base Superalloy 625: from Conventional Thermomechanical Processed to Selective Laser Melting Processed," *In Proceedings of Microscopy and Microanalysis 23* supplement S1(Cambridge University Press, Rio De Janeiro, 2017), pp. 2250-2251.
18. P. Richer, M. Yandouzi, L. Beauvais and B. Jodoin, "Oxidation Behaviour of CoNiCrAlY Bond Coats Produced by Plasma, HVOF and Cold Gas Dynamic Spraying," (Elsevier, Ottawa, 2014), pp. 3962–3974.
19. N. H. Sateesh, G. M. Kumar, K. Prasad, C. K. Srinivasa, A. R. Vinod, Microstructure and Mechanical Characterization of Laser Sintered Inconel 625 Superalloy," (Elsevier, Mangalore, 2014), pp. 772-779.